

Self-consistent renormalization group approach to continuous phase transitions in alloys. Application to ordering in β -brass

V I Tokar

Université de Strasbourg, CNRS, IPCMS, UMR 7504, F-67000 Strasbourg, France

E-mail: tokar@ipcms.unistra.fr

¹G. V. Kurdyumov Institute for Metal Physics of the N.A.S. of Ukraine, 36 Acad. Vernadsky Boulevard, UA-03142 Kyiv, Ukraine

Abstract. A self-consistent (SC) renormalization group approach of the effective medium kind has been developed and applied to the solution of the Ising model (IM). A renormalization group equation in the local potential approximation (LPA) derived previously for spatially homogeneous systems has been extended to the lattice case and supplemented with a self-consistency condition on the pair correlation function. To validate the approach it has been applied to the simple cubic IM and good agreement of the spontaneous magnetization calculated with the use of the SC-LPA equation with the available exact Monte Carlo simulations data has been established. Next the approach has been applied to the bcc IM corresponding to β -brass. With the use of the effective pair interaction parameters from available *ab initio* calculations the critical temperature, the correlation length and the long range order parameter in the vicinity of the critical point have been calculated in excellent agreement with experimental data. Qualitative and quantitative arguments have been given in support of the suggestion that the experimentally observed decrease of the effective critical exponent of the order parameter in comparison with the universal value is enhanced by the positive value of the second neighbour pair interaction found in the *ab initio* calculations.

Keywords: self-consistent renormalization group equation, local potential approximation, ordering in the Ising model, ordering in beta brass, critical temperatures, effective critical exponents of the order parameter

1. Introduction

Modern theory of alloys aims at describing the order-disorder phase transitions fully *ab initio* without resort to any phenomenological input [1]. However, because inclusion of correlated disorder in the band structure calculations meets with severe difficulties [2, 3], theoretical treatment of interatomic correlations at finite temperature is usually done in two steps. At the first step the configuration-dependent electronic structure energy is mapped onto the Ising model (IM) with the effective cluster interactions (ECIs) between the spins and at the second step the IM thermodynamics is treated by means of statistical mechanics [1, 4, 5, 6, 7, 8].

Currently no universal theoretical techniques efficient at both stages exist partly because different alloys may exhibit qualitatively different behaviour and a technique efficient in alloys of one kind performs poorly in alloys of different kind. In particular, cluster methods of [1, 9, 10] that proved to be efficient in the description of the first order phase transitions fail to correctly describe continuous transitions because small clusters cannot properly account for the long range correlations in the critical region. The cluster sizes N_c are restricted to small values because the number of terms in the equations grows as 2^{N_c} so in practical calculations cluster radii have to be bounded by a few lattice constants [1, 9, 10].

The restriction on the cluster sizes is greatly alleviated in the Monte Carlo (MC) method [11] where instead of all spin configurations, as in the analytical cluster theories, only a relatively small number of the most important configurations is explicitly simulated. As a consequence, the linear size L of the simulation box, the homologue of the clusters in the analytical approaches with $N_c \propto L^3$ in 3D, is limited only by available computational resources. A major advantage of the MC approach is that it can treat IM of any complexity. For example, in [5] the Hamiltonian corresponding to Ta-Mo alloy with ECIs consisting of eight pair and five many-body interactions was simulated in broad range of temperatures with the use of the simulation boxes with $L = 16 - 32$ lattice units. The simulations predicted, in particular, a yet unobserved continuous ordering transition with the critical temperature T_c in the range 600–1000 K. The poor accuracy in T_c determination was due to an unusually broad maximum in the specific heat curve. Obviously that the critical behaviour of the specific heat was impossible to describe at this level of accuracy. But the problem was not only in the complexity of the Hamiltonian or in too small simulation boxes and insufficient statistics. Even on simple cubic (sc) lattice and IM with only NN interactions the simulations with box sizes up to $L = 1024$ l.u. it proved impossible to determine with good accuracy the specific heat critical exponent α [12]. In earlier study with $L \leq 512$ the error in determination of α was $\sim 100\%$ [13].

Still, because other critical exponents were quite accurately determined in the simulations in [14, 13, 12], the MC approach in principle can be used for the description of experiments on ordering in β -brass in [15] because specific heat was not measured in the study. However, the MC simulations needed may require quite extensive computations in

order, for example, to determine differences between the values of the critical exponent of the order parameter β in different experimental set-ups and/or models. In experiments in [15] the difference in β values that we would like to explain was less than 4%. But in [13], where according to the authors the MC data of unprecedented size were simulated, β could be determined with the accuracy of only $\pm 2.5\%$, so the error in the difference between two values of β would exceed the difference $< 4\%$ we are interested in.

Much better accuracy was achieved in recent simulations in [12] but at the cost of 2×10^7 CPU core hours (2.3 thousand years) on five Linux clusters. Rough estimates show that for the accuracy which would be sufficient for the present study these numbers could be reduced. But it should be taken into account that instead of one nn model on sc lattice studied in [12] three different models on bcc lattice with additional next nn interactions in two of them would need to be simulated. In view of the discussion in the previous paragraph it should be concluded that large-scale computations would still be necessary.

The extensive MC simulations seems to be the only practical way to reliably calculate thermodynamic quantities in the critical region in the case of Hamiltonians containing many-body ECIs that usually arise in realistic descriptions of the configurational alloy energy [1, 4, 5, 6, 7, 8]. However, in some alloys the energy can be described with the use of only pair interactions, in particular, β -brass is considered to be such an alloy [15, 6]. In this case the partition function can be represented in the form of a functional integral over a scalar lattice field with the field Hamiltonian formally of the Ginzburg-Landau type with conventional non-local quadratic (“free”) part and a local interaction potential (see, e.g., [16, 9, 10]). The critical behaviour of the models of this type can be effectively treated within the functional renormalization group (RG) approach, in particular, within the local potential approximation (LPA) [17, 18, 19, 20].

The aim of the present paper is to derive a RG equation in the LPA based on the self-consistent functional formalism developed in [16, 9, 10]. Though unlike the MC method this approach is not universal and systematic, it has some important advantages. First, it can be formulated directly in the thermodynamic limit, so no need for repeated simulations with different L values with subsequent non-trivial interpolation to the infinite system size needed in MC simulations in the critical region [14, 13, 12]. Second, the pair interactions of any extent can be treated in exactly the same manner as nn interactions. Third, the critical behaviour can be described within well established RG framework so the universality properties and scaling laws hold for all periodic lattices, unlike in MC simulations where their validity is not guaranteed [13]. Furthermore, the cluster MC algorithms that are needed in large-scale simulations to overcome the critical slowdown degrade their performance in the presence of competing interactions [21]. But such interactions are ubiquitous in metallic alloys where they arise due to the Friedel oscillations of the electron density [7, 8, 5]. In the proposed RG approach such interactions would not pose any complications, as will be seen in the calculations in the *ab initio* IM of β -brass with competing nn and next nn interactions [6]. Finally, the RG equation in the LPA is computationally undemanding and can be solved on practically

any computer.

The equation will be obtained by modification of the RG equation in the LPA derived in [22] for the Ginzburg-Landau model in homogeneous space. The modification will consist in adaptation of the equation to the lattice case and in imposing the self-consistency condition similar to that used in [16, 9, 10]. The equation that will be called the SC-LPA RG equation belongs to the class of nonperturbative RG equations in the LPA [17, 18, 19, 20] and shares their known shortages. In particular, the universal quantities, such as the critical exponents, are approximately reproduced in the LPA in 3D case but not in 2D; the non-universal quantities, such as the critical amplitudes, are accurate to the lowest order in the interaction but in the strong coupling case that will be of main interest in the present study the SC-LPA should be considered as a heuristic closed-form approximation. Formally it is analogous [16] to such successful approximation as the coherent potential approximation (CPA) and DMFT [2, 23] which in the strong coupling case can be justified only in some limiting cases (e.g., in infinite dimensions) but have been successfully applied to many physical problems. Therefore, before proceeding to the description of β -brass we will first check and validate the SC-LPA RG equation by comparing its predictions with known reliable solutions of similar problems in [14, 24, 25].

2. Formalism

In the pair approximation the configuration-dependent contribution to the total energy of an equiatomic binary alloy in the IM formalism reads [1, 6]

$$E_{conf} = \frac{1}{8} \sum_{ij} V_{ij} s_i s_j \quad (1)$$

where $s_i = \pm 1$ are the Ising spins occupying N lattice sites $\{i\}$ and V_{ij} are the effective pair interactions which following [6, 15] we will restrict to only the nearest neighbour (V_1) and the second neighbour (V_2) interactions which is sufficient for the discussion of ordering in β -brass [24, 6, 15]. In (1) linear in s_i terms are absent because the transformation $s_i \rightarrow -s_i$ corresponds to replacement of atoms of one kind by the atoms of another kind and in the equiatomic alloy this should not change the configurational energy. In the IM language this means that the external magnetic field is equal to zero. On bipartite lattices, such as the simple cubic (sc) and the bcc lattices, this additionally makes possible to switch the signs of spins $s_i \rightarrow -s_i$ on one of the two interpenetrating sublattices and simultaneously reverse the signs of V_{ij} connecting spins at different sublattices to arrive at a model with the same statistical properties but with different order parameter [24]. In the case under consideration the antiferromagnetic order will change to the ferromagnetic one and because the ferromagnetic order is simpler, in the study of ordering in β -brass (bcc lattice) we will deal with the transformed system. To avoid confusion, V_1 and V_2 will retain their physical values while in explicit calculations

we will use the dimensionless (i.e., divided by $k_B T$) Hamiltonian of the form

$$H_I = \frac{1}{2} \sum_{ij} \epsilon_{ij} s_i s_j - \sum_i h_i s_i + N \epsilon_0 / 2 \quad (2)$$

with the interactions between the nn and the second neighbour spins $\epsilon_1 = -V_1/4k_B T$ (note the sign reversal) and $\epsilon_2 = V_2/4k_B T$, respectively. Besides, we introduced into ϵ_{ij} a diagonal part $-\epsilon_0 \delta_{ij}$ with

$$\epsilon_0 = \frac{-8V_1 + 6V_2}{4k_B T} \quad (3)$$

which is compensated by the last term in (2)) because of the identity $s_i^2 = 1$. This is done to ensure the quadratic behaviour of the Fourier-transformed ϵ at small momenta [24]

$$\epsilon(\mathbf{k})|_{\mathbf{k} \rightarrow 0} \simeq \frac{V_1 - V_2}{k_B T} a^2 \mathbf{k}^2 \quad (4)$$

where a in the bcc case was chosen to be equal to one half of the length of the cube edge so that the vectors connecting nn sites have coordinates $(\pm a, \pm a, \pm a)$ and their length $a_1 = \sqrt{3}a$ (in the sc case the cube edge and the nn distance coincide).

Besides, in (2) we added the linear coupling of spins to the source field h that will be needed, e.g., in the formulation of the self-consistency condition. At the end of the calculations, however, it will be set equal to zero because only the equiatomic alloys and the IM in zero external field will be studied in the present paper.

The calculations below will be based on the SC approach of the effective medium type introduced in [16]. Because the formalism was recapitulated in several papers (see, e.g., [9, 10, 26]) only its one-component variant sufficient for IM will be briefly explained below. The derivation of the SC condition is based on the observation that the conventional in the many-body theory separation of the Hamiltonian into the quadratic (or harmonic) in the fluctuating field part and an interaction part which is of higher order in the field is not unique. An arbitrary quadratic term can be added to the harmonic part and simultaneously subtracted from the interaction part which would leave the Hamiltonian unchanged. The reason for this transformation is that the harmonic part defines the propagator of the perturbation theory and the arbitrary term can in principle be adjusted so that the propagator was equal to the exact pair correlation function of the field which arguably is the most useful and most often calculated correlation function in the many-body theory.

In the functional-integral representation the partition function of the Ising model (2) reads

$$Z[h] = e^{N\epsilon_0/2} \prod_l \int ds_l 2\delta(s_l^2 - 1) e^{-\frac{1}{2} \sum_{ij} \epsilon_{ij} s_i s_j + \sum_i h_i s_i} \quad (5)$$

where the delta functions fix the continuous spins s_i to their Ising values ± 1 . By standard manipulations [16, 9, 10, 26] (5) can be cast in the form (see, e.g., equations (5) and (6) in [16])

$$Z[h] = \exp\left(\frac{1}{2} h G h\right) R[Gh] \quad (6)$$

where the vector-matrix notation has been used in the N -dimensional space of the lattice sites so that, e.g., $Gh = \sum_j G_{ij}h_j$, etc. The propagator matrix G is translationally-invariant and its Fourier transform reads

$$G(\mathbf{k}) = \frac{1}{\epsilon(\mathbf{k}) + r}. \quad (7)$$

Here momentum-independent constant r plays the role of the SC self-energy in the single-site cluster approximations [16, 9, 10, 26]. In the IM case it can be introduced into (5) in the same manner as ϵ_0 in (2) with the corresponding compensating term accounted for in (6) through

$$\begin{aligned} R[s] &= \det(2\pi G)^{1/2} e^{N(r-\epsilon_0)/2} \exp\left(\frac{\partial}{\partial s} G \frac{\partial}{\partial s}\right) \prod_l [2\delta(s_l^2 - 1)] \\ &= \exp\left(\frac{\partial}{\partial s} G \frac{\partial}{\partial s}\right) \exp(-U^b[s]). \end{aligned} \quad (8)$$

Here we introduced the “bare” or initial local potential

$$U^b[s] = \sum_i u^b(s_i) \quad (9)$$

which will be renormalized by the RG procedure and in the LPA is assumed to remain local throughout the whole course of renormalization [22].

2.1. Connection with polynomial models

From (8) it follows that in the case of the IM $u^b(x)$ in (9) formally contains a poorly defined contribution of the form

$$u^b(x) = -\ln \delta(x^2 - 1) + (\text{f.i.t.}) \quad (10)$$

where by (f.i.t.) we denoted field- or x -independent terms. This will not pose problems in the calculation below because, as shown in Appendix A, in the differential RG equation we can use $\exp(-u^b)$ instead of u^b so in explicit calculations only the plain delta-function will appear. However, in the Wilson theory [17] the local potential u^b in (9) is usually assumed to be a polynomial function of its argument. The IM expression (10) is very far from the polynomiality and even the analyticity. This poses the question on whether the results of the conventional RG approach that heavily relies on the perturbative expansions requiring the analyticity of u^b apply to the IM. The possibility that IM is exceptional from the RG standpoint has been discussed in the literature and large-scale MC simulations have been performed in support of this viewpoint (see [13, 27] and references therein).

The “layer-cake” renormalization scheme makes possible to reformulate the above question for the case of lattice models with local interactions as follows. As has already been discussed in [28, 26] (see, e.g., section 4.2 in [28]), in the lattice case the partial initial renormalization that has led to our equations (A.12) and (A.14) can be performed exactly because it amounts to application of the site-diagonal operator $\exp[(t_0/2)\partial^2/\partial s_i^2]$

to the factors $\exp[-u^b(s_i)]$ in (8) individually at each site. The exact expression thus obtained reads

$$R[s] = \exp\left(\frac{\partial}{\partial s}\tilde{G}\frac{\partial}{\partial s}\right)\exp\left[-\sum_i u(s_i, t_0)\right] \quad (11)$$

where u is defined in (A.11) and (A.12) and

$$\tilde{G}_{ij} = G_{ij} - t_0\delta_{ij} \quad (12)$$

where the second term on the right hand side is subtracted because it has already been accounted for in the partial renormalization.

Expression (11) is exact and is amenable to treatment by means of the perturbation theory because due to the integration in (A.12) the IM now is represented by u in (A.14) which can be expanded in a convergent Taylor series. For polynomial theories, e.g., for the conventional ϕ^4 the initial function u calculated in (A.11) and (A.12) will also be representable as the infinite Taylor series so on the same lattice and the same dispersion ϵ the difference between IM and ϕ^4 theories will be only in the coefficients of the expansion of the local potential at time t_0 . Thus, there seems to be no reasons why the critical properties as described by the RG would be different in the two cases. Therefore, in the present paper we assume that the RG theory is fully applicable to IM. This assumption presumes, in particular, that the MC simulations of IM on the largest lattices used today cited in [13] are not able to correctly describe the critical behaviour.

2.2. The self-consistency condition

As follows from (5), the spin correlation function can be found by differentiating the logarithm of $Z[h]$ in (6) with respect to h_i twice which after setting h to zero gives in the matrix notation [16, 9, 10, 26]

$$\|\langle s_i s_j \rangle\| = G - G \frac{\partial^2 U[s]}{\partial s \partial s} G \Big|_{s=0}. \quad (13)$$

Because the exact partition function does not depend on r , the value of the latter can be chosen arbitrarily. In approximate calculations, however, the independence will usually be lost in which case r can be used as a free parameter to improve the approximation. In effective medium theories, one aims at choosing r in such a way that the second term in (13) disappeared and propagator G coincided with the exact correlation function. This would mean that the propagation of an individual (quasi)particle within the medium is unperturbed by the scattering described by the second term, hence the term ‘‘effective medium’’.

In general, however, it is impossible to set the second term in (13) to zero with the use of a single parameter because in this case r would coincide with the exact self-energy $r^{exact}(\mathbf{k})$ of the system which in non-trivial models depends on \mathbf{k} . With only one momentum-independent parameter at hand the effective medium condition can be satisfied only approximately. In the single-site approximation it is assumed that in the exact renormalized potential $U^R[s] = -\ln R[s]$ (here and below we will designate

by superscript R all fully renormalized quantities) the site-diagonal terms dominate so similar to (9) U^R can be approximated by a sum of local potentials $u^R(x)$ and the condition

$$u_{xx}^R|_{x=0} = 0 \quad (14)$$

will nullify the second term in (13) locally which roughly corresponds to assuming the site-local self-energy $r \approx r_{ii}^{exact}$.

However, in studying the critical region one is interested mainly in the behaviour of the long range fluctuations, so with only one free parameter being available it seems more logical to impose the self-consistency condition on the self-energy at the smallest value of the momentum $r \approx r^{exact}(\mathbf{k} \rightarrow \mathbf{0})$. As will be shown below, in our SC RG approach this will amount to imposing condition (14) on the local potential u^R obtained as the solution of the LPA RG equation.

2.3. The SC-LPA RG equation

Finding the partition function (6) is equivalent to calculating functional R in (8). But for our purposes it will be sufficient to find only the function of the homogeneous field $h_i = h = Const$ which in (6) will be replaced by $Gh = h/r$ (see (7)). Of course, before doing this substitution all partial derivatives in (8) should be taken.

Calculation of the derivatives in (8) by means of a RG technique in the LPA has been explained in detail in [22] (cf. our equation (8) with equation (4) in [22]). A slight difference with the present case is that in [22] all Fourier components $s_{\mathbf{k}}$ were set to zero while now we want to preserve the component with $\mathbf{k} = \mathbf{0}$. This is trivially achieved in equation (8) in [22] by simply not setting to zero the argument of the fully renormalized local potential $u^R(x)$ because after successive elimination of all higher-momenta components the remaining x corresponds to $s_{\mathbf{k}=\mathbf{0}}$. In the present study $x = h/r$ will be retained in order to calculate the dimensionless free energy per site in the external homogeneous field h needed in the derivation of further thermodynamic quantities

$$f(h) = -\ln Z = u^R(x)|_{x=h/r} - h^2/2r. \quad (15)$$

Here the use has been made of equations (6), (7), (8) and (9).

More serious problem to resolve is that in [22] the RG equation was derived for statistical models in homogeneous isotropic space. Though it is not difficult to adopt the ‘‘layer cake’’ renormalization scheme of [22] to lattice models [26], in the present paper we adopt another possibility based on the observation made in [29] in the theory of the single-site CPA. Namely, in [29] it was shown that for any single-band density of states (DOS) it is possible to construct rotationally-invariant dispersion $\tilde{\epsilon}(k = |\mathbf{k}|)$ that would reproduce it. But in [30, 26] it was found that the LPA RG equations depend on the lattice structure only through the DOS corresponding to dispersion $\epsilon(\mathbf{k})$. This means that it should be possible to apply to lattice systems the LPA equations derived for the isotropic space. The only problem is that the isotropic dispersion is not uniquely defined [29]. However, as we show in Appendix A, $\tilde{\epsilon}$ can be completely excluded from

the LPA equation of [22] by a change of the evolution parameter from the momentum cut-off Λ to “time” t defined in (A.4) thus avoiding the ambiguity. Specifically, by substituting (A.3) and (A.8) in (A.1) one gets

$$u_t = \frac{1}{2} [p(t)u_{xx} - u_x^2]. \quad (16)$$

where the subscripts denote the partial derivatives and

$$p(t) = D_{tot}(t^{-1} - r) = \int_0^{t^{-1}-r} dE D(E) \quad (17)$$

in complete agreement with $n = 1$ lattice case in [26]. We note that in the ferromagnetic case under consideration the integration over t in (16) is bounded from above because $D(E)$ in (17) vanishes at negative E where dispersion $\epsilon(\mathbf{k})$ is equal to zero so when t exceeds r^{-1} , $p(t)$ also turns to zero. Thus, unlike in more conventional LPA approaches [18, 20] in [22] and in the SC LPA the evolution spans a finite interval of t values except at the critical point where $t_{max} = r^{-1}$ becomes infinite.

The RG equation in the LPA (16) with the initial condition (A.14) and the self-consistency condition (14) constitute the SC-LPA RG scheme that will be used in explicit calculations throughout the present paper.

Equation (16) could be readily integrated numerically in the symmetric phase above T_c . Below T_c , however, insurmountable numerical difficulties have been encountered. The problem has been attributed to the exact quadratic partial solution (the Gaussian model) which in the coexistence region below T_c becomes negative and singular at some point $t_{sing} > 0$:

$$u^G(x, t) = \frac{x^2}{2(t - t_{sing})} + (\text{f.i.t.}) \quad (18)$$

At $t = 0$ the initial curvature in solution (18) is negative and diverges to $-\infty$ as $t \rightarrow t_{sing}$. The integration cannot go beyond this point because the singularity is non-integrable, so it was identified with the end point of the integration $t_{sing} = 1/r$. The singularity, however, is not a deficiency of the LPA. In fact, it ought to be expected on physical grounds because the magnetic susceptibility should be infinite in the coexistence region but according to (5) and (15) it is given by the second derivative

$$\chi = d^2 \ln Z / dh^2|_{h=0} = 1/r - u_{xx}^R|_{h=0}/r^2. \quad (19)$$

And because r in (19) is proportional to the squared inverse correlation length $r \propto \xi^{-2}$ it should be finite both above and below T_c . Hence, the infinite susceptibility can arise only from the second term so its unboundedness is dictated by the physics of the problem.

The physical soundness of the approximation is gratifying but we have to find a way of dealing with the singularity. In view of the direct connection between u and the free energy (15), a plausible idea would be to resort to a Legendre transform (LT) of $u(x)$, say, $v(y)$, because under the transform the second derivatives of v and u would be inversely proportional to each other [31] and the infinity in u_{xx} would turn into numerically manageable zero in v_{yy} . This general idea has been realized in a non-canonical way via a LT-like t -dependent transform explained in Appendix B which for

simplicity we will continue to call the LT transform. Equations (B.1) and (B.2) have been obtained as a generalization of the t -independent LT suggested in [32] (see also [18]). Though our LT does not have the canonical form [31], it solves the singularity problem because the transformed LPA equation

$$v_t = \frac{p(t)v_{yy}}{2(1 + \bar{t}v_{yy})} \quad (20)$$

($\bar{t} = t - t_0$) obtained from (B.4) and (B.5) has a Gaussian solution with a t -independent quadratic in y term which thus is non-singular in t . In the coexistence region where $t_{sing} = 1/r$ the LT-transformed (18) reads

$$v_G(y, t) = -\frac{y^2}{2\bar{t}^R} + (\text{f.i.t.}) \quad (21)$$

where $\bar{t}^R = 1/r - t_0$. With the use of (B.5) susceptibility (19) expressed in the $v - y$ variables is

$$\chi = \frac{1}{r} - \frac{v_{yy}^R}{r^2(1 + \bar{t}^R v_{yy}^R)} \Big|_{h=0}. \quad (22)$$

As is seen, though the solution (21) in the coexistence region is finite, the susceptibility in (22) is infinite, as needed.

It is to be noted that (18) and (21) are only particular solutions of the RG equations and there is no obvious reason why they should dominate the solution for arbitrary non-Gaussian models, especially taking into account that in the disordered phase the solution u or v for the IM are non-Gaussian. Nevertheless, in the numerical solutions of the IM in the coexistence region the y -dependent part of v^R was indistinguishable from v^G within the accuracy of the calculations which was $O(10^{-6})$ in our case (see Appendix C). This is illustrated in figure C1.

A minor inconvenience of dealing with the LT variables v and y is that they do not have an obvious physical meaning. But in view of (B.3) the transform can be easily inverted, so that at the end of the integration we have

$$x = h/r = y + \bar{t}^R v_y^R \quad (23)$$

$$u^R = v^R + \bar{t}^R v_y^2/2. \quad (24)$$

Thus, in view of (15), both the field and the free energy can be represented in parametric form in terms of y and v so other thermodynamic quantities can be expressed through y and v with the use of the standard thermodynamic relations.

The discussion of the LPA solution below T_c will be continued in section 4 but first let us consider the simpler disordered phase.

3. Disordered phase

Using the IM language, in experiments above T_c in [15] the authors measured the spin-spin correlation function and compared it with that calculated in [24] for the nn bcc IM.

In slightly modified notation (a_1 instead of a), expression (11.1) for the susceptibility in [24] reads

$$\hat{\chi}(\mathbf{k}, T) = \frac{(a_1/r_1)^{2-\eta}}{[(\kappa_1 a_1)^2 + a_1^2 K^2(\mathbf{k})/(1-\eta/2)]^{1-\eta/2}}. \quad (25)$$

Definitions of quantities entering this expression can be found in [24] so here we only note that κ_1 is the inverse correlation length ξ^{-1} and that r_1 in (25) is unrelated neither to our r nor to the nn sites.

In the LPA the susceptibility is given by $G(\mathbf{k})$ (7) which, in particular, means that $\eta = 0$ [18, 22] and in this approximation it should coincide with (25). To cast the two expressions in the same form we first multiply the numerator and the denominator of (7) by a_1^2 and note that $K^2(\mathbf{k})$ in (25) was defined in [24] as our $\epsilon(\mathbf{k})$ but normalized so that at small k it behaved as k^2 with the coefficient unity. In view of (4) this means that (7) will acquire the form of (25) if we further divide the numerator and denominator by $(V_1 - V_2)a^2/k_B T$. By comparing the numerators one finds that in the LPA:

$$\left(\frac{a_1}{r_1}\right)^2 \simeq \frac{3k_B T}{V_1 - V_2} = \frac{3T^r}{4(1 - V_2/V_1)} \quad (26)$$

where use has been made of the fact that $(a_1/a)^2 = 3$ and for simplicity we introduced the dimensionless temperature

$$T^r = \epsilon_1^{-1} = (V_1/4k_B T)^{-1}. \quad (27)$$

Similar comparison of the first terms in the denominators gives

$$(\kappa_1 a_1)^2 = (a_1/\xi)^2 \simeq 3T^d r/4(1 - V_1/V_2). \quad (28)$$

The values of parameters in (25) were given by expressions (9.9) and (9.14) in [24]:

$$\log_{10} \kappa_1 a_1 \simeq \nu \log_{10} \tau + B_0 + B_1 \tau \quad (29)$$

and

$$r_1(T)/a_1 = (r_1/a_1)_c(1 - c\tau + \dots), \quad (30)$$

respectively, where $\tau = |1 - T/T_c|$ and other parameters are listed in tables VI and VII in [24].

For quantitative comparison, the SC-LPA equation (20) was solved numerically for nn bcc IM in the vicinity of T_c in the disordered phase. Details of the numerical techniques used are given in Appendix A. The results are compared with the solution of [24] in figure 1 and in table 1. As is seen, the largest discrepancy is between the values of B_1 . But because in (29) B_1 is multiplied by τ , at the largest value of τ in Fig. 1 it introduces the error amounting to only about 1% of B_0 . As a result, in this range the discrepancy between the LPA values of ξ and the values calculated on the basis of (29) with the parameters from Table VI in [24] is smaller than 3%. When $\tau \rightarrow 0$ the error becomes negligible so the discrepancy seen in the figure at small τ should be attributed to the difference in ν , as can be seen from a steeper LPA curve. Thus, with the overall discrepancy in a few percent the agreement can be deemed to be satisfactory taking into

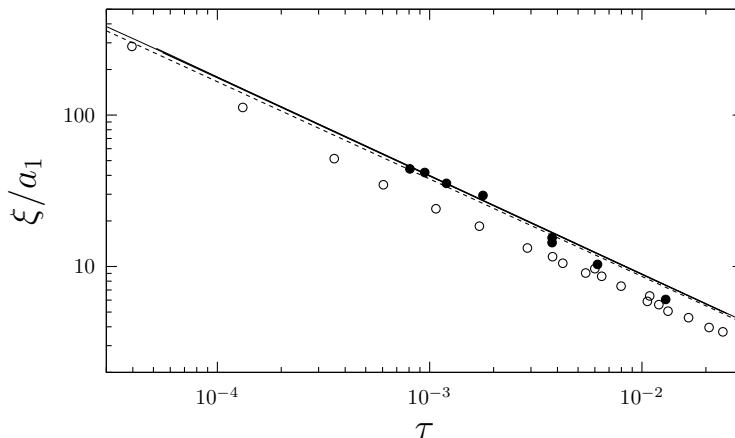


Figure 1. Correlation length above T_c : dashed curve and the empty circles were calculated as $(\kappa_1 a_1)^{-1}$ on the basis of (29) with the parameters from [24] and from the experimental data of Fig. 10 in [15], respectively; three overlapping solid lines are the LPA solutions for the nn IM and for the IM with $V_1 = 3.8$ mRy and two second neighbour interactions $V_2 = 0.9$ mRy [6] and -1 mRy; the black circles are experimental data from Fig. 9 in [15].

Table 1. Comparison of the parameters entering expressions (29) and (30) for nn Ising model on bcc lattice as calculated in the present work and in [24] (tables VI and VII). For simplicity, all numbers were rounded so as that the discrepancy between the two approaches were in one significant figure.

	ν	B_0	B_1	η	$(r_1/a_1)_c$	c	$(a_1/r_1)_c^{2-\eta}$
LPA	0.65	0.352	-0.3	0	0.46	0.50	4.75
[24]	0.64	0.351	-0.1	0.06	0.45	0.47	4.77

account that the authors assess the accuracy of (25) in 12% [24]. Besides, the LPA T_c agreed with the best known estimates for T_c in the nn bcc IM within 0.3% [26].

It is reasonable to assume that the accuracy of the LPA similar to the nn case will also hold for IM with not too large second neighbour interactions. This is further confirmed by the fact that $T_c \simeq 748.5$ K calculated with the *ab initio* values of the interactions taken from Fig. 1 in [6] $V_1 = 3.8$ mRy and $V_2 = 0.9$ mRy differed from the experimental value 739 K on 1.3% which is appreciably larger than 0.3%. This discrepancy can be a consequence of the further neighbour interactions neglected in [6]. The correlation length calculated with these parameters is also shown in figure 1 and is almost indistinguishable from the nn case. This means that according to our calculations the model can describe the experimental data in disordered phase as well as the nn model but, in addition it can predict T_c with reasonable accuracy and, besides, has a firm *ab initio* foundation [6].

To complete the check on the influence of the next neighbour interactions on the behaviour of the correlation length, a model with negative V_2 has been solved and also did not show appreciable deviations from the nn case. Thus, our calculations do not support the suggestion made in [33] that farther-neighbour interactions can be

responsible for disagreement of the nn model with experimental data.

4. Ordered phase

The behaviour of the order parameter below T_c measured in β -brass in [15] is more difficult to interpret quantitatively. Theoretically, in a close vicinity of the critical point the order parameter follows the power law

$$m_0^*(\tau) = a_0^* \tau^{\beta^*}, \quad (31)$$

where the order parameter m_0 , the amplitude a_0 and the critical exponent β have been starred because in the finite temperature range they do not correspond to the true critical quantities but only to the effective ones that are influenced by the corrections to scaling and cannot be defined independently of the experimental set-up in which they were measured.

In the Ising universality class the order-disorder transitions are described by the universal critical order parameter exponent which value according to the most advanced MC simulations is [14, 13, 34, 12]

$$\beta \simeq 0.325 \pm 0.002. \quad (32)$$

In this paper we will neglect distinctions between the true universal value, the value β found in [14] and $\beta^{LPA} = 0.325$ because their differences are negligible on the scale of variation of β^* in our calculations and in [15] where (31) fitted to experimental data in two temperature intervals gave the following values

$$\beta^* = 0.313, \quad \tau \lesssim 0.014 \quad (33)$$

$$\beta^* = 0.29 \pm 0.01, \quad \tau \lesssim 0.04 \quad (34)$$

which disagree with (32) in the second and even in the first significant digit. Moreover, (33) and (34) violate the scaling relation $\beta = \nu(1 + \eta)/2$ holding in 3D [35] because with $\nu = 0.64$ adopted in [15] the universal value of β should exceed 0.32 for any $\eta > 0$.

The above discrepancies should be expected because the power laws with the universal exponents are strictly valid only asymptotically when $\tau \rightarrow 0$ and cannot describe data on finite temperature intervals where the true behaviour is different from (31) and in 3D case is unknown. Rigorous RG theory predicts an infinite number of correction terms of the power-law type with known exponents but not amplitudes [36]. Thus, expression (31) is not valid on any finite temperature interval and the quantities entering it do not have much physical meaning so they were marked by the stars to distinguish them from the physical spontaneous magnetisation m_0 , the critical amplitude a_0 and the universal critical exponent β that will be calculated below with the use of the SC-LPA RG equation.

Nevertheless, because in [15] some experimental data were fitted to (31), below we discuss peculiarities of such a fit with the reservation that fitting to an incorrect expression is a poorly defined problem and the fit results will depend on practically all details of the fitting procedure, such as the distribution of the measured points, their

weights, etc. The main goal pursued by the nonperturbative RG approach is to calculate all quantities of interest directly without the need to resort to heuristic expressions of unknown validity.

As explained in Appendix C, below T_c two quantities should be determined self-consistently within the SC LPA approach: self-energy r and the spontaneous magnetisation m_0 . With known $v^R(y)$ the latter according to (5), (15), (B.3) and (23) can be calculated as

$$m_0 = y_0 - t_0 v_y^R|_{y_0} = y_0 / (1 - r t_0) \quad (35)$$

where the last equality was obtained from (23) for $h = 0$. But for general $h \neq 0$ the first equation in (35) should be used.

Because the phases above and below T_c are physically quite different, in the absence of quantitative criteria of the accuracy of the approach the SC-LPA solution should also be tested in the ordered phase by comparing it with reliable reference data. To this purpose the highly accurate MC simulations in the ordered phase made in [14] have been used. Though the model studied was the nn sc IM, similar to bcc the sc lattice is bipartite and its coordination is only 25% smaller so the accuracy of LPA in this system should be similar to what can be expected in the bcc case.

4.1. Ordering on the sc lattice

The results of the MC simulations in [14] were summarized in the form of an interpolation formula

$$m_0(\tau) = \tau^\beta (a_0 - a_1 \tau^\theta - a_2 \tau) \quad (36)$$

where the precise parameter values are given in [14]; the rounded values are given in table 2 below. In figure 2 magnetisation (36) is compared with the LPA calculations. The accuracy of expression (36) is quite high, of order of 10^{-5} [14] but the accuracy of the LPA calculations were at best $2 \cdot 10^{-3}$ at $m_0 = 1$ because of the finite differentiation step used. Therefore, in all our fits and figures the smallest m_0 was chosen to be 0.2 in order to have the accuracy at least not worse than 1%, though the LPA equation could be easily solved for much smaller magnetisations. Good accuracy of the data, however, is vital for our purposes because we intend to study quantitatively the deviations of the LPA data from the linearity in the region $\tau \leq 0.04$ where they are hardly discernible on the scale of the graph in figure 2. The non-linearity of the logarithm of $m_0(\tau)$ is, however, obvious from the fitting expression (36). To assess the quality of the LPA solution it was fitted to the LPA points in figure 2 with the use of the LPA order parameter exponent $\beta = 0.325$ and the leading correction exponent taken to be $\theta = 0.5$ [36] because the corrections to it are of higher order of the ε -expansion [17] than the LPA which is accurate only to the first order in ε [18, 22]. As can be seen from table 2, similar to the disordered case the worst agreement is with a correction term, this time with a_1 which is about one third smaller than the MC value. Still, the largest error in m_0 introduced by this discrepancy is about 3.6% at the maximum value of $\tau = 0.26$. It

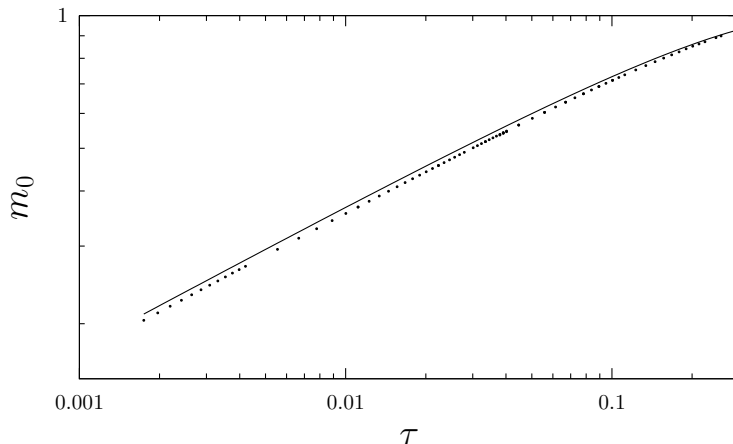


Figure 2. Spontaneous magnetisation in the sc IM: solid line—the interpolation of the exact MC simulations (36) [14], symbols—the LPA solution.

Table 2. Parameters of the LPA $m_0(\tau)$ fit to (36) with β and θ held fixed compared to rounded values from [14].

	T_c	β	θ	a_0	a_1	a_2
LPA	4.475	0.325	0.50	1.62	0.22	0.41
[14]	4.512	0.327	0.51	1.69	0.34	0.43

is even smaller at 0.04 and shrinks to zero as $\tau \rightarrow 0$. This, however, is an important difference to us because of the strong influence of the leading correction on the effective order parameter exponent β^* [35].

In [15], however, the data were fitted not to (36) but to more conventional power law (31) so let us find out how accurately the SC-LPA reproduces such fits. As was already pointed out, in the fit to an incorrect function all details of the fitting procedure may influence the results. Therefore, because in [15] the authors fitted a quantity proportional to m_0^2 , in checking the reliability of SC-LPA we fitted the squared power law (31) to the squared MC data (36) by minimizing the integral

$$I = \int_{\tau_0}^{\tau} [m_0^*(\tau')^2 - m_0(\tau')^2]^2 d\tau' \quad (37)$$

with respect to a_0^* and β^* . In (37) it is implicitly assumed that all data have the same weight and, besides, are homogeneously distributed within the interval $[\tau_0, \tau]$. These assumptions, of course, are rather arbitrary but they will allow us to roughly estimate the span of variation of possible values of β^* .

The integrals in (37) can be calculated analytically and the parameters found exactly. The fitted values of β^* are shown in figure 3 by the solid lines. The upper line corresponds to the fit when the lower limit of integration in (37) was held fixed at τ_0^{\min} corresponding to $m_0 = 0.2$ while the upper limit varied from τ_0 to $\tau^{\max} = 0.04$. At the lower line the upper limit was fixed while τ_0 varied from τ_0^{\min} to τ^{\max} . This case roughly imitates the situation when the data at small m_0 are given very low weight

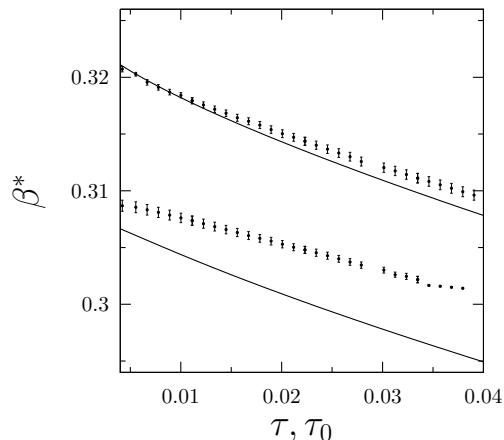


Figure 3. The effective order parameter exponent β^* fitted to the MC (solid lines) and to the LPA (symbols) simulation data. For details of the fitting procedure see the text.

because of larger errors.

Similar procedure was applied to the LPA data except that instead of the integral the sum over discrete points was used in the expression for I . As can be seen in figure 3, the agreement with the fit to MC data is not perfect and the LPA values show smaller deviations from the universal β . This reflects the smaller amplitude of the leading correction a_1 noted above. But it should be born in mind that the deviation of β^* from β that we are interested in is less than 10% and in the worst case of agreement the LPA still predicts $\sim 80\%$ of it. The important conclusion from these fits is that the deviations are similar in magnitude to those obtained experimentally and so potentially may explain them if the bcc case exhibits deviations of similar magnitude.

4.2. Ordering on bcc lattice.

Thus, judging from the sc IM, the accuracy $\sim 20\%$ may be expected in the LPA deviations of the effective exponent β^* in the bcc case shown in figure 4. The simulations were carried out for the same models as in section 3 but this time the difference between the three cases was clearly visible, though it was not large.

The important observation that can be made from figure 4 is that the fits seem to support the *ab initio* model of [6] in comparison with the nn IM ($V_2 = 0$) used in the interpretation of experimental results in [15]. The difference between the two cases, however, is rather small, not exceeding the LPA errors estimated in the sc case so the question arises of whether the difference is real. Because the observation is one of the main results of the present study, below are given qualitative arguments in favour of the conclusion that $\beta^*(V_2 > 0)$ should indeed be smaller than $\beta^*(V_2 = 0)$.

To begin with, let us consider a ferromagnetic IM with interactions of the form

$$\epsilon_{i \neq j} = C(\lambda)e^{-|i-j|/\lambda} \quad (38)$$

where $|i - j|$ is the Euclidean distance between the sites, λ is a characteristic interaction

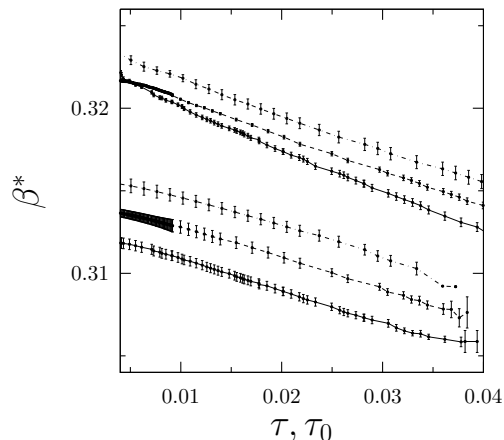


Figure 4. The upper and the lower groups of curves were obtained in as in figure 3. The simulated models were the same as listed in the caption to figure 1; the solid line corresponds to $V_2 = 0.9$ mRy, dashed line to $V_2 = 0$ and dashed-dotted line to $V_2 = -1$ mRy.

range and $C < 0$ can be chosen so as to keep the critical temperature fixed, though the latter is not obligatory. It is important to note that the nn IM belongs to the class of models (38) with $\lambda \rightarrow 0$. As is known, in the limit $\lambda \rightarrow \infty$ model (38) tends to the exactly solvable mean-field (MF) model with all $\epsilon_{i \neq j}$ being equal and the critical exponent $\beta_{MF} = 0.5$. The latter, however, holds only when $\lambda = \infty$. At any finite λ the model belongs to the same Ising universality class as the nn IM but as λ grows the true critical region shrinks and outside of it the MF behaviour dominates. Thus, when fitted to the power law (31) within a finite temperature interval the effective β^* should grow from its initial value close to 0.3 corresponding to nn IM (see figure 4) toward the MF value 0.5.

Model (38) is of interest to us because our model with $V_2 = -1$ mRy can be accurately represented by (38). Indeed, with $|V_2/V_1| \approx 0.26$ and the distances between the second and the first neighbours differing on $\simeq 0.27a$, the effective interaction range can be found to be $\lambda \simeq 0.2a$. The third neighbour interaction in this case according to (38) has the strength $\sim 1.6\%$ of V_2 so to a good approximation $V_{l \geq 3}$ can be neglected. Obviously, the models with negative V_2 but with smaller $|V_2|$ can be approximated by (38) even better. Now, because in the short-range ferromagnetic models belonging to the Ising universality class, there is no other critical or otherwise singular points, it should be expected that the behaviour of $\beta^*(\lambda)$ would be monotonous with larger λ meaning larger β^* .

Thus we have shown that for a finite temperature interval near T_c and the models with only nn and the second neighbour interactions the effective order parameter exponent fitted at this interval should monotonously diminish from the value $\beta^*(V_2 = -1$ mRy) toward $\beta^*(V_2 = 0)$. Now by continuity arguments it can be concluded that when V_2 grows farther by acquiring positive values the decrease of β^* should persist which qualitatively agrees with the fits shown in figure 4. Of course, if V_2

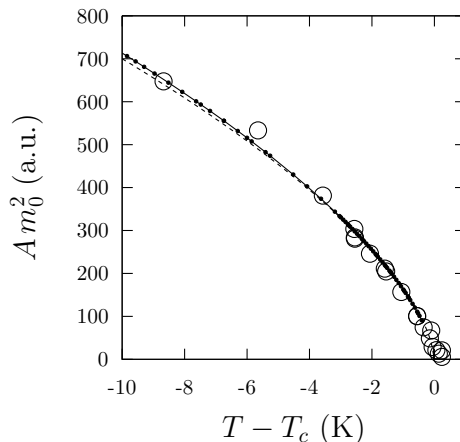


Figure 5. The empty circles and the dashed curve are, respectively, the experimental data and their power-law fit (31) with $\beta^* = 0.313$ taken from Fig. 6 in [15]. The black dots (connected by solid line for better visibility) are the LPA results adjusted to the data via parameter A .

becomes sufficiently large to cause the frustration effects the continuity may fail. But $V_2 = 0.9$ mRy is rather small in comparison with $V_1 = 3.8$ mRy so the continuity arguments should hold.

4.3. Ordering in β -brass.

The values of fitted β^* shown in figure 4 indicate that the experimentally observed behaviour of the order parameter for $\tau \lesssim 0.014$ interpolated in [15] by the power law (31) with $\beta^* = 0.313$ should be amenable to description by the SC-LPA equation with the *ab initio* parameters V_1 and V_2 as in [6]. Indeed, as shown in figure 5, in this region the LPA calculations compare well with the experimental points and the power law curve from [15]. This, however, does not mean that both descriptions are equally adequate. In contrast to the phenomenological theory of [15], in the RG approach the problems with the universality and the scaling relations do not arise [17, 35] and the LPA preserves these features, though with approximate values of critical exponents ($\beta^{LPA} = 0.325$ and $\nu^{LPA} = 0.65$) [18, 22, 20]. The small deviations from the best known values are expected to be corrected in the future with the use of techniques developed in the theory of nonperturbative RG [19]. Our use of the rotationally-invariant formalism to describe lattice models should considerably facilitate the task. But the main advantage of the SC-LPA is that there is no need in heuristic expressions to fit experimental data because all observable quantities can be calculated directly.

Farther from T_c , however, in the interval $\tau \lesssim 0.04$ the experimentally found value $\beta^* = 0.29 \pm 0.01$ can hardly be reproduced in the LPA because the effective beta range in figure 4 extends from ~ 0.305 upwards. The LPA values of m_0^2 calculated at the seven τ points close to those in the inset in Fig. 11 in [15] fitted to the power law (31) have given $\beta^* \approx 0.315 \pm 0.002$ which is noticeably greater than (34). Because LPA overestimates

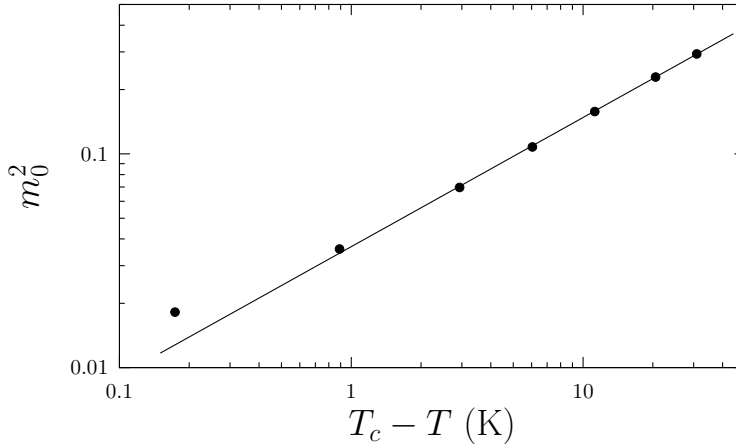


Figure 6. LPA data points (symbols) shifted on $\simeq 0.2$ K toward T_c fitted to power law (31) (solid line) with $\beta^* \simeq 0.30$; experimental points at these temperatures were fitted in [15] with $\beta^* \simeq 0.29 \pm 0.01$.

β^* , the real discrepancy may be smaller but if the sc case is representative of what may be expected on the bcc lattice, the downward shift of β^* in figure 3) would be too small to explain the remaining discrepancy $\Delta\beta = 0.025$.

Thus, the value of effective $\beta^* = 0.29$ cannot be quantitatively understood within the model with parameters of [6]. Two possible explanations for this failure can be envisaged. First, at $\tau = 0.04$ the calculated long range order parameter reaches as large value as 0.53 which may influence the interatomic interactions propagated via the electronic subsystem and thus change the values of V_1 and V_2 as well as introduce additional effective cluster interactions.

The explanation may also lie in the experimental uncertainties in the temperature measurement in [15] which according to the authors were of the order of 0.2 K. To assess possible implications, let us assume that away from T_c the measured temperatures were systematically overestimated so that they were effectively shifted toward the critical temperature being about $\Delta T \approx 0.2$ K closer to T_c than they were in reality. Alternatively, this may be a consequence of the error in determination of T_c , or errors of both kinds could contribute to the shift. Now by fitting the same seven LPA points as above to the re-defined $\tau = 1 - (T + \Delta T)/T_c$ in (31) one finds $\beta^* = 0.302 \pm 0.005$ which already overlaps with (34). Taking into account that LPA overestimates the effective exponents the agreement with experiment may be even better. As can be seen in figure 6, qualitatively the fit looks as good as the corresponding fit in [15] except at the point closest to T_c . But this point is one of the many in the vicinity of T_c which are rather scattered due to the steepness of the order parameter in this region and the perfect agreement of the point with the fitting curve could be accidental.

5. Conclusion

In this paper a SC RG equation in the LPA has been derived and applied to an accurate quantitative description of the MC simulation data on the magnetic ordering in the sc lattice [14] and to experimental data on the ordering in β -brass [15]. In the latter case it has been shown that with the use of the *ab initio* values of the effective pair interactions [6] it has been possible to calculate the critical temperature T_c with $\sim 1\%$ accuracy and describe the critical behaviour in the 1.4% vicinity of T_c satisfying the universality principle and the scaling relations between the critical exponents. These features were lacking in the phenomenological theory in [15] based on the approximate solution of the nn IM [24].

In the sc case it has been found that in the SC-LPA the order parameter is accurately described within the distance $\gtrsim 25\%$ away from T_c . Therefore, the inability of the theory to reproduce the observed effective critical exponent β^* at the distance $\sim 4\%$ from the critical point has led to the conclusion that either the model parameters are strongly influenced by the order that could exceed the value 0.5 in this range, or that the temperatures were systematically overestimated within the accuracy of the measurements ~ 0.2 K or both factors contributed to the discrepancy. Further research would be needed to clarify this issue.

In this paper the RG equation has been derived for the simplest case of the scalar field which is sufficient for the treatment of the Ising model. The equation in [22], however, was derived for the general n -vector model with local interactions in the homogeneous space. It can be easily shown that similar to the scalar case the SC-LPA RG equation for the lattice n -vector models can be derived along the lines of the present paper. In fact, this equation has already been derived in [28, 26] within the functional renormalization scheme in the reciprocal space of the lattice momenta. This more complicated formalism can be necessary for the calculation of corrections to the LPA. But within the LPA the simple approach of renormalization in homogeneous momentum space is sufficient for recovering all concrete results and calculations of [28, 26].

The most serious deficiency of the LPA-based approach is that it cannot be rigorously justified beyond the perturbation theory which is a common problem in all strongly coupled many-body and field-theoretic models. Strong coupling, however, is frequently encountered in physical systems which was the reason for the development of heuristic theories dealing with it. Arguably, among lattice models the most thoroughly investigated are the CPA and the DMFT (see the bibliography on these methods in review articles [2, 23]). It is remarkable that, as shown in [16], these and some other strong coupling approximations can be derived within the same formalism and with the effective medium self-consistency condition similar to that used in the present paper. This suggests that in approximations of this kind there exists some underlying mechanism of attenuation of the corrections. This assumption is supported by the excellent agreement of many experimental and MC data with the CPA [2, 37, 38] and with the SC-LPA [26]. Moreover, non-local corrections to the CPA in a strongly

disordered tight-binding model alloy calculated in [39] on the basis of the expansion suggested in [16] were found to be in excellent agreement with the exact MC simulations, thus justifying and improving the CPA in this particular case. Besides, cluster generalizations of the single-site theories have been actively developed and promising results obtained [9, 23, 10, 40]. So there is a good deal of hope that further research along these lines will make possible to set effective medium theories on a firm theoretical footing.

Appendix A. LPA for lattice models

The LPA RG equation (16) in the main text can be obtained from the RG equation derived in [22] as follows. First, in the case of a one-component field corresponding to the IM equation (8) in [22] reads

$$\frac{\partial u}{\partial \Lambda} = \frac{1}{2} \frac{dG}{d\Lambda} \left[\left(\frac{\Lambda}{\Lambda_{BZ}} \right)^3 \frac{\partial^2 u}{\partial x^2} - \left(\frac{\partial u}{\partial x} \right)^2 \right] \quad (\text{A.1})$$

where u is the local potential, Λ the momentum cut-off, x the local field and the propagator

$$G(\Lambda) = \frac{1}{c(\Lambda)} = \frac{1}{\tilde{\epsilon}(\Lambda) + r}, \quad (\text{A.2})$$

where c is the coefficient of the quadratic in the field part of the Hamiltonian in [22] which for easier comparison with (7) is convenient to separate into the dispersion term $\tilde{\epsilon}(\Lambda)$ behaving as $\sim \Lambda^2$ when $\Lambda \rightarrow 0$ and the momentum-independent self-energy r . Besides, we explicitly included in (A.1) the maximum cut-off momentum Λ_{BZ} , where BZ stands for the ‘‘Brillouin zone’’. In [22] Λ_{BZ} was set equal to unity but because in the present paper we want to apply the equation to arbitrary lattices, the size of BZ should also be arbitrary. Also, this factor corrects the equation from the dimensionalities standpoint.

By substituting (A.2) into (A.1) one obtains the equation that explicitly depends on the rotationally-invariant dispersion $\tilde{\epsilon}(\Lambda)$ which according to [29] can be fitted to the DOS of a lattice model thus enabling application of (A.1) to lattice systems. In general the fit is not unique [29] but, fortunately, in the case of equation (A.1) this difficulty can be overcome by a change of the evolution variable. To show this let us first divide both sides of the equation by $dG/d\Lambda$ and on the basis of definition

$$dt = \frac{dG}{d\Lambda} d\Lambda = dG \quad (\text{A.3})$$

introduce the new independent variable

$$t = G = \frac{1}{\tilde{\epsilon}(\Lambda) + r}. \quad (\text{A.4})$$

Because all quantities here are positive, t is bounded from above by the maximum value $1/r$ reached when $\tilde{\epsilon} = 0$.

In (A.1) Λ is now a function of t which formally can be found from (A.4) as

$$\Lambda(t) = \tilde{\epsilon}^{-1}(t^{-1} - r) \quad (\text{A.5})$$

where $\tilde{\epsilon}^{-1}$ is the function inverse to $\tilde{\epsilon}(\Lambda)$.

The explicit dependence of Λ in (A.1) on t can be found with the help of the integral

$$\Lambda^3(t) = \int_0^{\Lambda_{BZ}} k^3 \delta[\tilde{\epsilon}^{-1}(t^{-1} - r) - k] dk. \quad (\text{A.6})$$

which after integration by parts can be transformed to

$$\begin{aligned} \Lambda^3(t) &= 3 \int_0^{\Lambda_{BZ}} k^2 \theta[\tilde{\epsilon}^{-1}(t^{-1} - r) - k] dk \\ &= 3 \int_0^{\Lambda_{BZ}} \theta[t^{-1} - r - \tilde{\epsilon}(k)] k^2 dk, \end{aligned} \quad (\text{A.7})$$

where on the first line the boundary terms were omitted by assuming that the first term in the argument of θ -function is smaller than Λ_{BZ} and on the second line we further assumed that $\tilde{\epsilon}(k)$ is a monotonous function. Though the integrand in (A.7) is isotropic, it can be integrated over all three components of \mathbf{k} by considering $\tilde{\epsilon}$ as a function of $k = |\mathbf{k}|$. Now the coefficient of the second derivative in (A.1) can be cast in the form convenient for generalization to the lattice case:

$$p(t) = \left(\frac{\Lambda(t)}{\Lambda_{BZ}} \right)^3 = \frac{1}{V_{BZ}} \int_{BZ} d\mathbf{k} \theta[E - \tilde{\epsilon}(\mathbf{k})] \Big|_{E=t^{-1}-r} \quad (\text{A.8})$$

where $V_{BZ} = 4\pi\Lambda_{BZ}^3/3$. As is easily seen, the last expression is just the integrated DOS of the quasiparticle band with dispersion $\tilde{\epsilon}$:

$$D_{int}(E) = \int_0^E D(E') dE' \quad (\text{A.9})$$

where $D(E)$ is the DOS corresponding to $\tilde{\epsilon}$ and, by construction, to $\epsilon(\mathbf{k})$. In this way $\tilde{\epsilon}$ can be totally excluded from equation (A.1).

Thus, we have shown that the rotationally invariant G from [22] and our lattice G lead to the same LPA RG equation provided $D(E)$ is the same. This makes possible to establish connection between the partition functions in both cases. By comparing our equations (6) and (8) with equation (4) in [22] for $n = 1$ one sees that our U^b differs from H_I in [22] only in terms that are constant in the field and “time” variables. But the LPA equations depend only on the derivatives so the constant terms in the free energy are unchanged by the renormalization and can be accounted for at any stage. Below they will be gathered into one expression (A.14) to facilitate their analysis.

Incidentally, (A.8) is also valid for $E > \max \tilde{\epsilon}$, that is, above the upper edge of the DOS in which case the theta-function is equal to unity so the integrated DOS of a filled band is unity. The values of E in this range are needed to integrate the RG equation in the range where t in (A.4) changes from zero to the minimum value of $G(\Lambda_{BZ} = 1)$ (see Fig. 1 in [22]):

$$0 \leq t \leq t_0 = \min_{\Lambda} G = (r + \max_{\Lambda} \tilde{\epsilon})^{-1} = [r + \max_{\mathbf{k}} \epsilon(\mathbf{k})]^{-1} \quad (\text{A.10})$$

Because $p(t) = 1$ is constant in this range, substitution

$$u = -\ln w \quad (\text{A.11})$$

reduces the RG equation to the diffusion equation which is integrated from $t = 0$ to t_0 with the use of the Gaussian diffusion kernel as

$$w(x, t_0) = (2\pi t_0)^{-1/2} \int dy e^{-(x-y)^2/2t_0} e^{-u^b(y)} \quad (\text{A.12})$$

This solution is particularly useful in the IM case where according to (8) and (9) the “bare” initial local potential

$$\exp[-u^b(x)] = \det(2\pi G)^{(1/2N)} e^{(r-\epsilon_0)/2} [\delta(x-1) + \delta(x+1)] \quad (\text{A.13})$$

is singular and difficult to deal with numerically. Substituting (A.13) in (A.12) one gets after some rearrangement

$$\begin{aligned} u(x, t_0) &= \frac{x^2}{2t_0} - \ln \cosh \frac{x}{t_0} - \ln 2 \\ &+ \frac{1}{2}(\epsilon_0 + \epsilon_{max}) + \frac{1}{2N} \ln \det \frac{r + \epsilon}{r + \epsilon_{max}} \end{aligned} \quad (\text{A.14})$$

It is to be noted that because by assumption $\tilde{\epsilon}(k)$ and $\epsilon(\mathbf{k})$ have the same DOS, the maxima of both dispersions which define its upper edge should be the same by construction. Also, the same DOS means the same spectrum and the eigenvalues density which means the same determinants in both cases. So in the initial condition (A.14) $\tilde{\epsilon}(k)$ can be replaced by its lattice homologue.

The usefulness of gathering all constants in $u(x, t_0)$ can be seen from the fact that the integration range of the SC-LPA equation $\bar{t}^R = 1/r - 1/(r + \epsilon_{max})$ scales as r^{-2} at large r , that is, in both limits $T \rightarrow \infty$ and $T \rightarrow 0$. Which means that in these limits $u(x, t_0) = u^R(x)$ so, for example, it is easy to see using (15) and (14) that in the $T \rightarrow \infty$ limit the SC-LPA predicts the exact reduced free energy $-\ln 2$. Further, by using (15), (23) and (C.2) it can be shown that $m_0 \rightarrow 1$ when $T \rightarrow 0$. Furthermore, at large r when the integration interval is small the SC-LPA equation can be integrated as a series in \bar{t}^R which can be further used to develop high- or low-temperature expansions of the solution for comparison with known results.

Appendix B. The Legendre transform

Appendix B.1. Regularization of equation (16)

To avoid dealing numerically with non-integrable singularity in the solution (18) of equation (16) it was found sufficient to slightly modify the Legendre transform for LPA equations suggested in [32] (see also [18]). The modification consists in introducing t -dependence into the transform as

$$v(y, t) = u(x, t) - \frac{1}{2} \bar{t} u_x^2 \quad (\text{B.1})$$

$$y(x, t) = x - \bar{t} u_x(x, t) \quad (\text{B.2})$$

where $\bar{t} = t - t_0$ with t_0 defined in (A.10). This choice was made for convenience and in general any constant can be used instead of t_0 . The independent variables in (B.1) and (B.2) are x and t , v and y being their functions.

Now by comparing equations (B.1) and (B.2) differentiated with respect to x it can be seen that

$$v_y = u_x \tag{B.3}$$

if $y_x \neq 0$. Similarly, by differentiating the equations with respect to t one finds

$$v_t = u_t + \frac{1}{2}u_x^2 = \frac{1}{2}p(t)u_{xx} \tag{B.4}$$

where the second equality follows from (16). Finally, differentiating (B.3) with respect to x and substituting y_x obtained from (B.2) one arrives at the relation

$$u_{xx} = \frac{v_{yy}}{1 + \bar{t}v_{yy}} \tag{B.5}$$

which being substituted in (B.4) gives the transformed RG equation (20) in the main text.

Appendix C. Numerical procedures

The evolution equation (20) has been solved by the method of lines with the use of LSODE routine [41] for 2500 discretization points at the positive (due to the symmetry) y axis. The point separation was $\Delta y = 2 \cdot 10^{-3}$ which in [20] was shown to be already small enough to give accurate values of many quantities of interest. In the double precision code [41] the use of smaller Δy was plagued with instabilities which restricted the accuracy of calculations of m_0 to $O(\Delta y)$. The second derivatives have been approximated by the three-term central differences in the LPA equation and by four-term one-sided differences at the points nearest to the jump in figure C1 with the quadratic accuracy $O(\Delta y^2) \sim O(10^{-6})$ in both cases. Similar calculations performed in [20] within different renormalization schemes with the use of a quadruple precision software showed that the accuracy can be considerably improved. Besides, in calculations of [20] the behaviour of the second derivative of the renormalized local potential qualitatively similar to that shown in figure C1 was observed and its formal and physical features discussed in detail. In the present study we adopted the conclusion made in [20] that the discontinuity in the second derivative is physically correct and real, though a rigorous formal proof would be desirable.

The integrated DOS needed in $p(t)$ has been calculated by numerical integration over BZ in (A.8) with $\tilde{\epsilon}$ replaced by $\epsilon(\mathbf{k})$. The step size in the momentum integration was ~ 0.01 ($\pi/300$). The integration was performed twice with the integrand Fermi smeared at two small Fermi temperatures T_F and subsequently interpolated to $T_F = 0$. The integrations were performed at 300 energy points and spline-interpolated in between. To improve precision at the band edges the exactly known behaviour (4) was used. The accuracy of the approximations from the renormalization group standpoint has

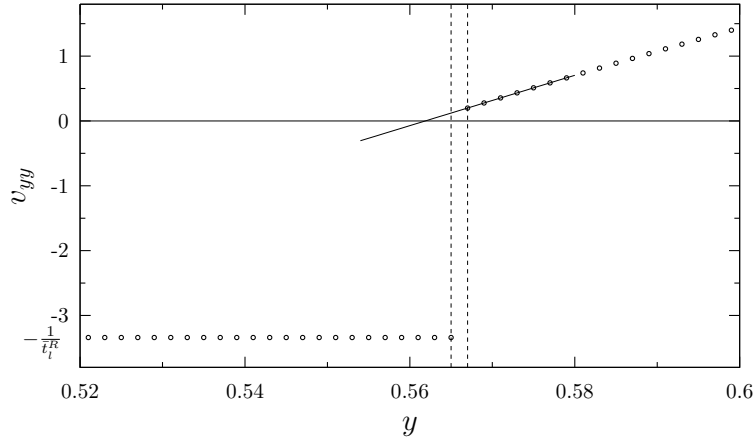


Figure C1. Circles: the second derivative of $v(y)$ calculated for the mn sc Ising model below T_c at an intermediate (l -th) iteration; $\bar{t}_l^R = 1/r_l - 1/(r_l + \epsilon_{max})$. As is seen, the derivative interpolated from the right of the jump interval bounded by vertical dashed lines does not turn to zero within the interval so further iterations are needed.

been checked by comparing the solutions of the LPA equation (20) obtained with the interpolated $p(t)$ and with the accurate analytical interpolation given in [42]. No noticeable differences were found.

The solution proceeded iteratively with the self-consistent r obtained as the limit of the recursion

$$r_{l+1} = r_l + v_{yy}^R|_{x=0} \quad (\text{C.1})$$

which converged when the self-consistency condition

$$v_{yy}^R|_{h+=0} = 0 \quad (\text{C.2})$$

was satisfied. According to (B.5) this is equivalent to the self-consistency condition (14) with h in (C.2) expressed through y according to (23). In the symmetric phase this simply means $y = 0$ but below T_c two stable solutions appear corresponding to $y = \pm y_0 \neq 0$ with the spontaneous magnetisation m_0 given by (35). So two conditions should be fulfilled below T_c : (C.2) and $h = 0$.

Acknowledgements

I express my gratitude to Université de Strasbourg and IPCMS for their hospitality. I am indebted to Hugues Dreyssé for support and encouragement.

This research did not receive any specific grant from funding agencies in the public, commercial, or not-for-profit sectors.

References

- [1] Ducastelle F 1991 *Order and Phase Stability in Alloys* (Amsterdam: North-Holland)
- [2] Elliott R J, Krumhansl J A and Leath P L 1974 *Rev. Mod. Phys.* **46** 465–543

- [3] Ziman J and Ziman P 1979 *Models of Disorder: The Theoretical Physics of Homogeneously Disordered Systems* (Cambridge University Press) ISBN 978-0-521-21784-2
- [4] Zunger A 1994 First-principles statistical mechanics of semiconductor alloys and intermetallic compounds *Statics and Dynamics of Alloy Phase Transformations (NATO ASI Series B: Physics vol 319)* ed Turchi P E A and Gonis A (New York: Plenum Press) pp 361–419
- [5] Blum V and Zunger A 2004 *Phys. Rev. B* **70** 055108
- [6] Turchi P E A, Sluiter M, Pinski F J, Johnson D D, Nicholson D M, Stocks G M and Staunton J B 1991 *Phys. Rev. Lett.* **67** 1779–1782
- [7] Asato M, Takahashi H, Inagaki T, Fujima N, Tamura R and Hoshino T 2007 *Mater. Trans.* **48** 1711–1716
- [8] Olsson P, Klaver T P C and Domain C 2010 *Phys. Rev. B* **81** 054102
- [9] Tokar V I 1997 *Comput. Mater. Sci.* **8** 8–15
- [10] Tan T L and Johnson D D 2011 *Phys. Rev. B* **83** 144427
- [11] Binder K 1986 *Monte Carlo Methods in Statistical Physics (Topics in Current Physics vol 7)* ed Binder K (Heidelberg: Springer-Verlag) p 1
- [12] Ferrenberg A M, Xu J and Landau D P 2018 *Phys. Rev. E* **97** 043301
- [13] Lundow P, Markström K and Rosengren A 2009 *Phil. Mag.* **89** 2009–2042
- [14] Talapov A L and Blöte H W J 1996 *J. Phys. A* **29** 5727
- [15] Madsen A, Als-Nielsen J, Hallmann J, Roth T and Lu W 2016 *Phys. Rev. B* **94**(1) 014111
- [16] Tokar V I 1985 *Phys. Lett. A* **110** 453–456
- [17] Wilson K G and Kogut J 1974 *Phys. Rep.* **12** 75–199
- [18] Bervillier C 2013 *Nucl. Phys. B* **876** 587
- [19] Berges J, Tetradis N and Wetterich C 2002 *Phys. Rep.* **363** 223 – 386
- [20] Caillol J M 2012 *Nucl. Phys. B* **855** 854–884
- [21] Blöte H, Heringa J and Luijten E 2002 *Comput. Phys. Commun.* **147** 58–63
- [22] Tokar V I 1984 *Phys. Lett. A* **104** 135–139
- [23] Maier T, Jarrell M, Pruschke T and Hettler M H 2005 *Rev. Mod. Phys.* **77** 1027–1080
- [24] Fisher M E and Burford R J 1967 *Phys. Rev.* **156** 583–622
- [25] Liu A J and Fisher M E 1989 *Physica* **156A** 35–76
- [26] Tokar V I 2019 Effective medium approach in the renormalization group theory of phase transitions (*Preprint* 1910.05123)
- [27] Deng Y and Blöte H W J 2003 *Phys. Rev. E* **68** 036125
- [28] Tokar V I 2019 Calculation of non-universal thermodynamic quantities within self-consistent non-perturbative functional renormalization group approach (*Preprint* 1904.10338)
- [29] Velický B, Kirkpatrick S and Ehrenreich H 1968 *Phys. Rev.* **175** 747–766
- [30] Machado T and Dupuis N 2010 *Phys. Rev. E* **82**(4) 041128
- [31] Zia R K P, Redish E F and McKay S R 2009 *Am. J. Phys.* **77** 614–622
- [32] Morris T 2005 *J. High Energy Phys.* **0507** 027
- [33] Dietrich O W and Als-Nielsen J 1967 *Phys. Rev.* **153** 711–717
- [34] Ron D, Brandt A and Swendsen R H 2017 *Phys. Rev. E* **95** 053305
- [35] Pelissetto A and Vicari E 2002 *Phys. Rep.* **368** 549–727
- [36] Wegner F J 1972 *Phys. Rev. B* **5** 4529–4536
- [37] Kissavos A E, Simak S I, Olsson P, Vitos L and Abrikosov I A 2006 *Comput. Mater. Sci.* **35** 1–5 ISSN 0927-0256
- [38] Kissavos A E, Shallcross S, Kaufman L, Grånäs O, Ruban A V and Abrikosov I A 2007 *Phys. Rev. B* **75** ISSN 1098-0121, 1550-235X
- [39] Tokar V I and Masanskiy I V 1987 *Fiz. Metall. Metalloved.* **64** 1207–1211
- [40] Tokar V I 2016 Hybrid cluster+RG approach to the theory of phase transitions in strongly coupled Landau-Ginzburg-Wilson model (*Preprint* 1606.06987)
- [41] Radhakrishnan K and Hindmarsh A C 1993 Description and use of LSODE, the Livermore solver for ordinary differential equations Tech. Rep. UCRL-ID-113855 LLNL

[42] Jelitto R. J 1969 *J. Phys. Chem. Solids* **30** 609–626